Supramolecular Chemistry
Vol. 25, No. 2, February 2013, 69–78

Taylor & Francis
Taylor & Francis Group

1,4-Diazobicyclo(2,2,2)octane-modified multi-ammonium derivatives as ratiometric fluorescent sensors for lipopolysaccharide

Wenwen Zhao[a,b], Jiasheng Wu[a], Weimin Liu[a] and Pengfei Wang[a]*

[a]*Key Laboratory of Photochemical Conversion and Optoelectronic Materials, Technical Institute of Physics and Chemistry, Chinese Academy of Sciences, Beijing 100190, P.R. China;* [b]*Graduate School of Chinese Academy of Sciences, Beijing 100049, P.R. China*

(*Received 30 June 2012; final version received 16 September 2012*)

A series of pyrene derivatives bearing multi-quaternary ammonium 1,4-diazobicyclo(2,2,2)octane groups were synthesised as ratiometric fluorescent sensors for lipopolysaccharide (LPS) in aqueous solution. Ratiometric changes in fluorescence spectra of the sensors were observed from the pyrene monomer–excimer conversion which is modulated by the supramolecular self-assembly between sensors and LPS. These sensors show high selectivity towards LPS with the detection limit down to tens of nanomolar levels. The interaction mechanism between the sensors and LPS was also discussed.

Keywords: lipopolysaccharide; pyrene; ratiometric; sensor; self-assembly

Introduction

Lipopolysaccharide (LPS, also known as bacterial endotoxin) is the main structural component in the outer cell membranes of all Gram-negative bacteria (*1*, *2*). It is responsible for the integrity and low permeability of the membrane, thereby protecting the bacteria from the destruction by antibiotics (*3*). But massive existence of LPS is an indication of bacteria contamination and can result in sepsis and septic shocks (*4*, *5*), which cause about 150,000 casualties annually in the USA (*6*). Due to its high toxicity of LPS, considerable efforts have been devoted to the development of specific quantification of LPS. Thus far, some analytical methods for LPS have been established including rabbit pyrogen test and enzymatic limulus amebocyte lysate (LAL) assay (*7*). However, there are some drawbacks for these methods, for instance, the rabbit pyrogen test shows low sensitivity and its result varies greatly with the individual differences in rabbits. The LAL assay is a sensitive method, whereas it is highly susceptible to changes in temperature and pH. Moreover, carbohydrate derivatives other than LPS, such as β-glucan, also respond positively in this assay (*8*). It is thus highly desirable to develop specific, quantitative and sensitive assays for detection of LPS.

Chromo- and fluorogenic chemosensors for biological species have attracted great attention due to their high sensitivity, good selectivity, as well as on-line and real-time analysis (*9*, *10*). However, only a few such sensors for LPS have been reported (*11–15*). Rangin and Basu (*11*) first reported a colorimetric sensor for LPS based on functionalised polydiacetylene liposome with the detection limit of about 100 μM, which is still much higher than the LPS toxic concentration (10^{-12} M). Recently, we have committed to the exploration of fluorescent sensors that can trace LPS *via* the lipophilic pyrene derivatives (*16*), cysteamine-modified gold nanoparticles (*17*) or co-polythiophene derivatives (*15*). These sensors exhibit high sensitivity with the detection limit at nanomolar or even picomolar levels.

LPS consists of a polysaccharide unit and a lipid A unit (Scheme 1a). The two phosphorylated glucosamine sugars in the lipid A and two 2-keto-3-deoxyoctanoate units, each carrying carboxylic groups, make LPS highly negatively charged. In addition, LPS is an amphiphilic molecule and can be automatically arranged in order in aqueous solution due to various long-chain fatty acid esters and amides attached to the glucosamine disaccharide core. Along with our continuing efforts in the exploration of fluorescent sensors for trace detection of LPS, we herein report a series of pyrene-based derivatives (**C_4-D-O-Py**, **C_2-D-O-Py**, **Ph-D-O-Py** and **C_2-D-Py**) bearing multi-ammonium 1,4-diazobicyclo(2,2,2)octane (DABCO) groups as ratiometric sensors for LPS in aqueous solution (Scheme 1b) *via* the supramolecular interactions. The introduction of two pyrene moieties into one molecular system is expected to detect LPS ratiometrically, which can effectively eliminate most or all interferences from the environment by built-in correction of two emission bands. Moreover, the multi-ammonium DABCO substituents in probes not only improve their water solubility but also provide four positive centres to bind with the negatively charged LPS *via* the strong electrostatic, hydrophobic and π–π stacking interactions. The most important differences among these probes are the connector flexibility between

*Corresponding author. Email: wangpf@mail.ipc.ac.cn

ISSN 1061-0278 print/ISSN 1029-0478 online

http://dx.doi.org/10.1080/10610278.2012.732224
http://www.tandfonline.com

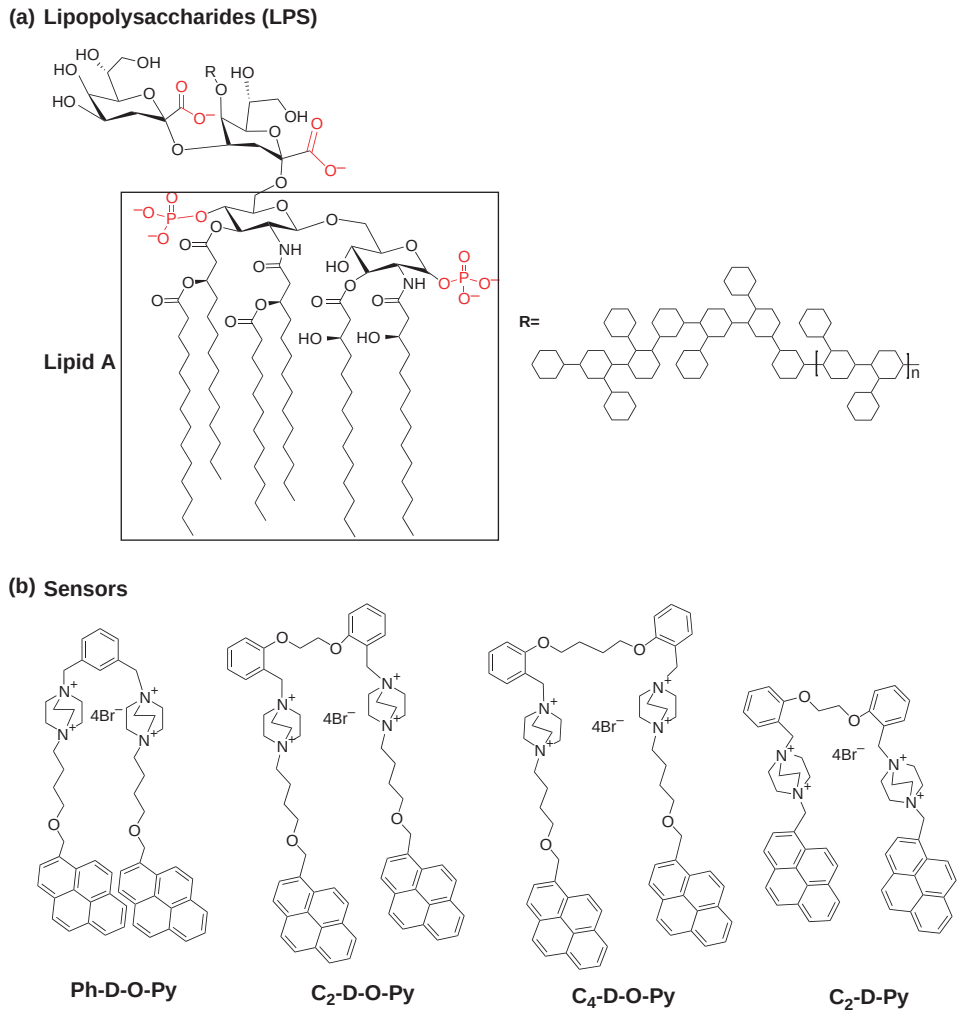

Scheme 1. Molecular structures of (a) LPS and (b) the sensors.

the two DABCO moieties and the alkyl chain length between DABCO and pyrene. It is found that the more flexible connector and the longer chain length of the sensor can help to improve the sensitivity and selectivity of the sensors to LPS.

Results and discussion

Synthesis and structural characterisation

The synthetic routes for fluorescent sensors are depicted in Scheme 2. Alkylation of *o*-methyl phenol with 1,2-dibromoethane or 1,4-dibromobutane afforded compounds **1** and **2**, which were further brominated with N-bromosuccinimide (NBS) to give dibromide derivatives **3** and **4**, respectively. Compounds **5** and **7** were synthesised according to the reported procedure, and then treated by DABCO to yield **6** and **8**. Finally, dibromide derivatives (**3**, **4** or *m*-xylylene dibromide) react with **6** or **8** to give the desired sensors with moderate yields (50–70%). All compounds were verified by ^{1}H, ^{13}C NMR and MS or element analysis. Details on the synthesis and characterisation are described in 'Experimental' section.

Optical spectral studies with LPS

Figure 1 shows the results of absorption spectra of **C_4-D-O-Py** (5 μM) in 4-(2-hydroacidxyethyl)-1-piperazineethanesulfonic acid (HEPES) buffer (10.0 mM, pH 7.4, H_2O:DMSO = 8:2, v/v) titrated with LPS. Without LPS, **C_4-D-O-Py** displays the absorption bands centred at 275, 327 and 343 nm. Upon addition of LPS ranging from 0 to 2.2 μM, band broadening and a significant red shift are observed, which can be attributed to the intermolecular π–π stacking of two pyrene groups in their ground state (Figure 1(a)) (*11*). Interestingly, the absorption intensity increases with a slight blue shift when LPS exceeds 2.6 μM (Figure 1(b)).

The excimer formation can be observed more directly from the fluorescence spectra (Figure 2). In the absence of

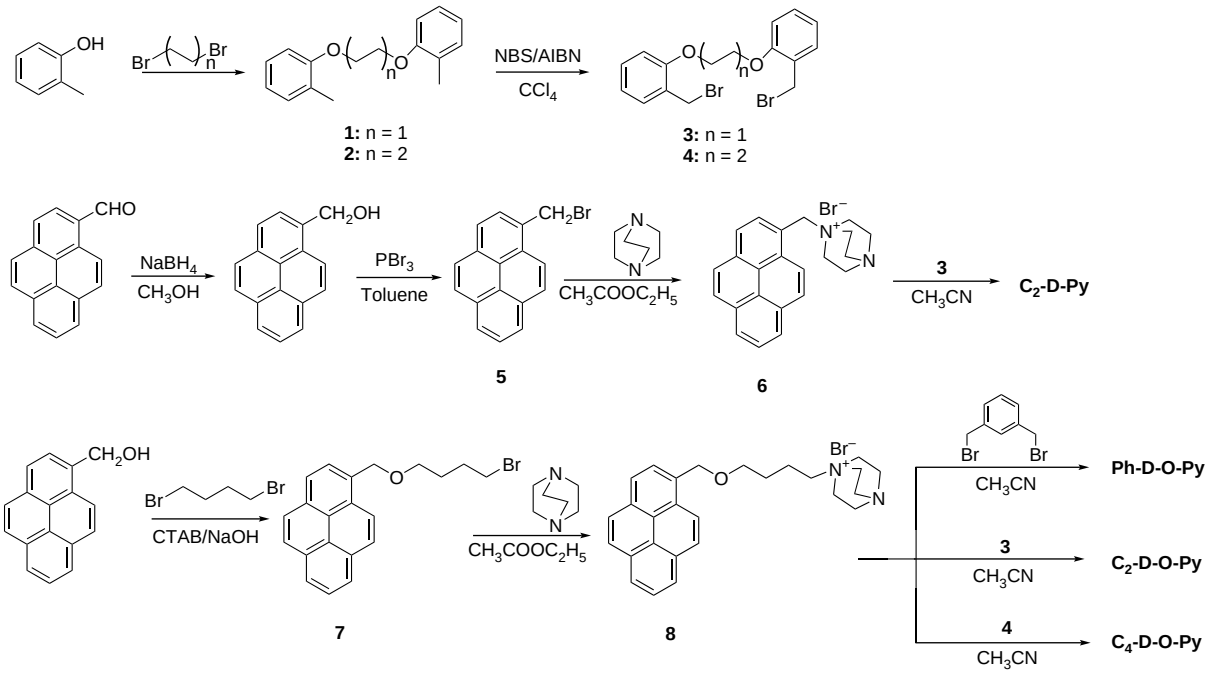

Scheme 2. The synthetic pathway of the sensors.

LPS, **C_4-D-O-Py** exhibits the emission peaks at 375 and 395 nm and a broad band centred at 489 nm. The former two are typical pyrene monomers and the last one corresponds to fluorescence emission of the excimer. Upon addition of 0–2.2 μM LPS, the fluorescence intensity of the monomer emission markedly decreases while the excimer emission intensity significantly increases with a discernible isoemissive point at 418 nm (Figure 2(a)). By plotting the emission intensity ratio (I_{485}/I_{389}) to the added LPS, a good linearity ($R^2 = 0.992$) was observed with the LPS concentration ranging from 0 to 1.8 μM (Figure 2(b)), indicating that the sensor **C_4-D-O-Py** enables ratiometric detection of LPS. The detection limits, defined as three times the standard deviation of the background, were calculated to be 18.5 nM, which is the lowest value of the reported LPS probes based on small organic molecules. When the concentration of LPS is further increased (2.6–25.2 μM), the fluorescence change reverses. This indicates that the monomer emission intensity increases dramatically, accompanied by a decrease in the excimer emission (Figure 2(c)). And the plot of I_{485}/I_{389} ratio to LPS concentration decreases gradually (Figure 2(d)).

Similar results were obtained with the addition of LPS to the solution of **Ph-D-O-Py** or **C_2-D-O-Py**. It can be seen that the band broadening and red shift in absorption spectra, and a significant excimer/monomer ratio enhancement in emission spectra were observed at low LPS concentration, whereas the optical spectra reverse at high LPS concentration (Figure S1 and S2 of the Supporting Information, available online, respectively). To clarify the effect of connector flexibility between two DABCO moieties on LPS sensing, we compared the responses of the three sensors

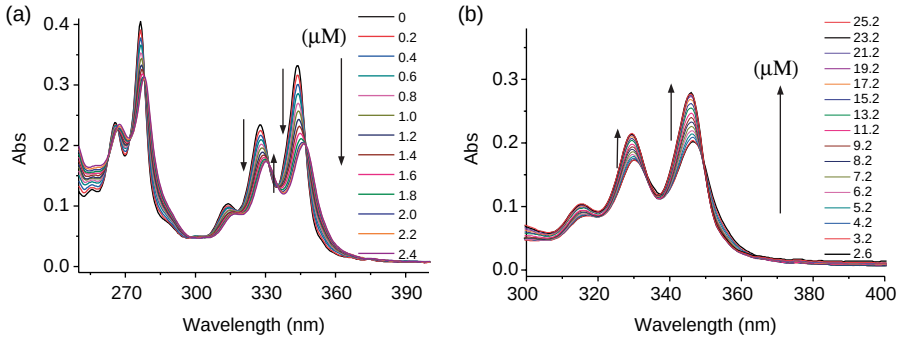

Figure 1. Absorption spectra of **C_4-D-O-Py** (5 μM) in the presence of different concentrations of LPS in a buffered (10 mM HEPES, pH 7.4, H_2O:DMSO = 8:2, v/v) solution: (a) 0–2.4 μM; (b) 2.6–25.2 μM.

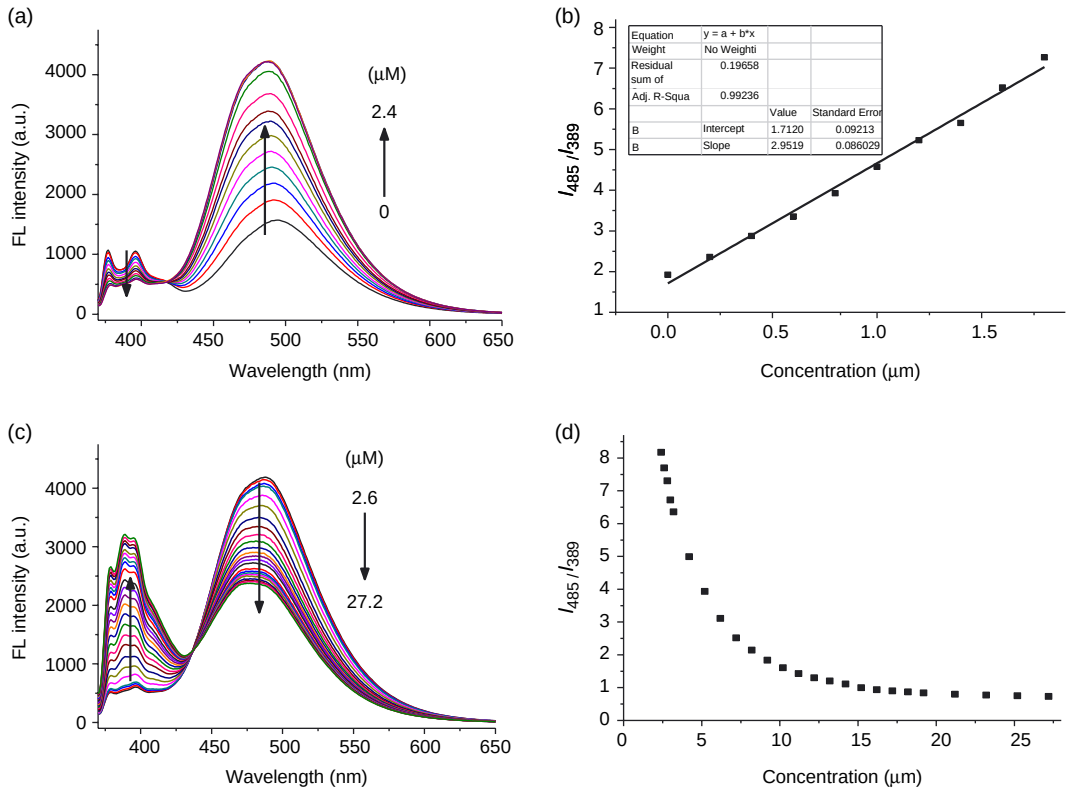

Figure 2. Fluorescence emission spectra (λ_{ex} = 360 nm) of **C_4-D-O-Py** (5 μM) recorded with different concentrations of LPS: (a) 0–2.4 μM; (c) 2.6–25.2 μM in a buffered (10 mM HEPES, pH 7.4, H_2O:DMSO = 8:2, v/v) solution; (b) and (d) fluorescence intensity ratio (I_{485}/I_{389}) against the LPS concentrations.

above to LPS, and the results are summarised in Figure 3 and Table 1. It can be seen that all of the three sensors can detect LPS by utilising the ratiometric signal of the excimer/monomer emission with tens of nanomolar detection limit, suggesting that the connector between the two DABCO moieties had a little effect on the spectral performance of the sensors. However, compared with **Ph-D-O-Py** and **C_2-D-O-Py**, **C_4-D-O-Py** with the maximal slope in the I_{485}/I_{389} ratio exhibits the lowest detection limit and the widest linear range. These results indicate that the more flexible of the connector between the two DABCO moieties, the better responses of the sensor towards LPS. Thus, the sensor **C_4-D-O-Py** was chosen for further discussion on pH effect and selectivity measurement.

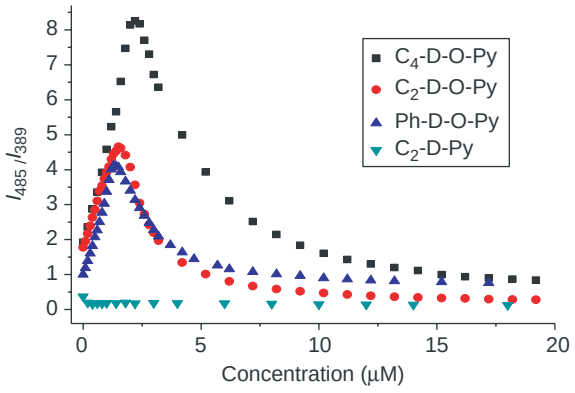

Figure 3. The fluorescence intensity in the I_{485}/I_{389} ratio of four different probes (5 μM) against the LPS concentrations in a buffered (10 mM HEPES, pH 7.4, H_2O:DMSO = 8:2, v/v) solution.

For the sensor **C_2-D-Py** in which the alkyl chain length between the DABCO and pyrene is shorter than that of the probes discussed above (**Ph-D-O-Py**, **C_2-D-O-Py** and **C_4-D-O-Py**), a distinctly different fluorescence response towards LPS was observed. As shown in Figure 4, the addition of LPS at even a higher concentration can give

Table 1. Summarised performance of the probes to LPS.

Compounds	The LPS concentrations corresponding to the increased I_{485}/I_{389} ratio (μM)	The linear range of LPS (μM)	Detection limit (nM)
C_4-D-O-Py	0–2.2	0–1.8	18.5
C_2-D-O-Py	0–1.6	0–1.3	25.2
Ph-D-O-Py	0–1.3	0–1.2	36.9

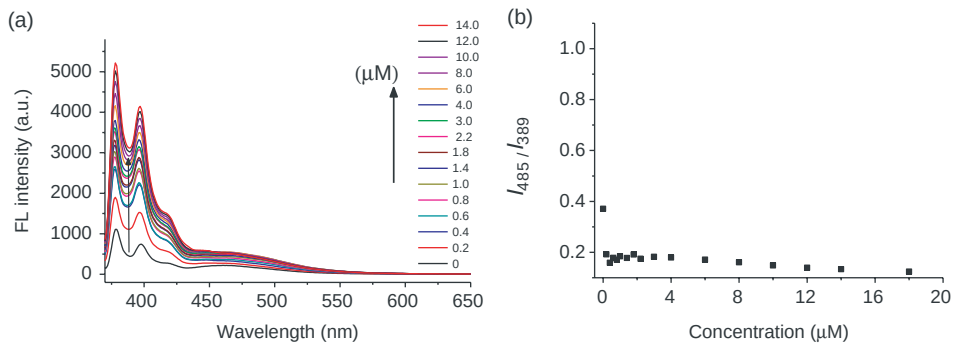

Figure 4. (a) Changes in fluorescent spectra ($\lambda_{ex} = 360$ nm) of **C_2-D-Py** (5 μM) upon addition of LPS in HEPES:DMSO (8:2, v/v) buffer solution (10 mM, pH 7.4). (b) Fluorescence intensity ratio (I_{485}/I_{389}) against the LPS concentration.

rise to a small change in monomer/excimer emission ratio, replaced by a significant increase in monomer emission. This could be attributed to the rigid conformation of DABCO groups which hinders the two pyrene groups close to form the excimer. This means that the sensors just with a flexible enough alkyl chain between DABCO and pyrene can detect LPS with a ratiometric change.

The proposed schematic illustration of the sensing mechanism for the probes to LPS is depicted in Scheme 3a. Without LPS, some molecules of **Ph-D-O-Py**, **C_2-D-O-Py** or **C_4-D-O-Py**, containing six bonds between DABCO and pyrene, exist in the monomer form in aqueous solution due to the relative rigid conformation of DABCO and the intramolecular electrostatic repulsion. Upon addition of low concentration of LPS, the strong electrostatic, hydrophobic and π−π stacking interactions could drive the probes and LPS to form supramolecular self-assembly, which weakens the intramolecular electrostatic repulsion and induces two pyrene moieties close to each other, thus leading to a significant increase in excimer/monomer emission ratio. Subsequently, with increasing concentration of LPS to a certain extent, the highly ordered phospholipids bilayers of LPS formed in aqueous solution may give rise to solubility enhancement, so that most pyrene moieties incorporate into micelle in monomer form. Moreover, the lower polarity inside LPS micelles reduces the possibility of an excited-state pyrene to encounter another ground-state pyrene. Those might be interpreted as the main reasons for the obvious decrease of excimer/monomer emission ratio at high LPS concentrations.

In contrast, although **C_2-D-Py** can also bind with LPS via strong electrostatic and hydrophobic interactions to form supramolecular self-assembly, no obvious excimer formations were found because the too short connector between DABCO and pyrene moiety cannot overcome the hindrance from rigid conformation of DABCO groups to form the excimer *via* the supramolecular interactions (Scheme 3b).

To further demonstrate the supramolecular self-assembly mechanism, the controlled experiments using **C_4-D-O-Py** treated with LPS in different solvents were carried out and the results are shown in Figure 5. Only in aqueous solution, **C_4-D-O-Py** exhibits a distinct spectral response to LPS (Figures 1 and 2), whereas in absolute DMSO, it cannot give rise to any spectral changes even at a higher LPS concentration (8.0 μM) (Figure 5), indicating that supramolecular self-assembly indeed plays an important role for LPS sensing.

pH effect

The effect of pH on the sensing performance to LPS was investigated. Taking **C_4-D-O-Py** for example, the fluorescence intensity I_{485}/I_{389} ratios of free sensor are relatively stable in a wide pH range from 3 to 11. However, the I_{485}/I_{389} ratios show an obvious pH dependency upon addition of LPS at a constant concentration of 2.5 μM. As shown in Figure 6, at acidic conditions, the I_{485}/I_{389} ratio drops a lot with decreasing pH. This phenomenon can be attributed to the carboxylate and phosphate (Pi) moieties of LPS may be partially protonated, which decreases the electrostatic interactions between the sensor and LPS. When pH ranges from 7 to 10, **C_4-D-O-Py** shows the highest fluorescence response towards LPS and the I_{485}/I_{389} ratios vary slightly with the pH changes. Therefore, a physiological condition of pH 7.4 (10 mM HEPES buffer) was chosen as the optimum determining medium for LPS sensing.

Selectivity

The selectivity of the sensors for LPS was evaluated by monitoring the fluorescence intensity ratio (I_{485}/I_{389}) response in the presence of various anions and biological species. We still take **C_4-D-O-Py** as an example, and the results are illustrated in Figure 7. It reveals that only the addition of LPS could result in a prominent increase of the

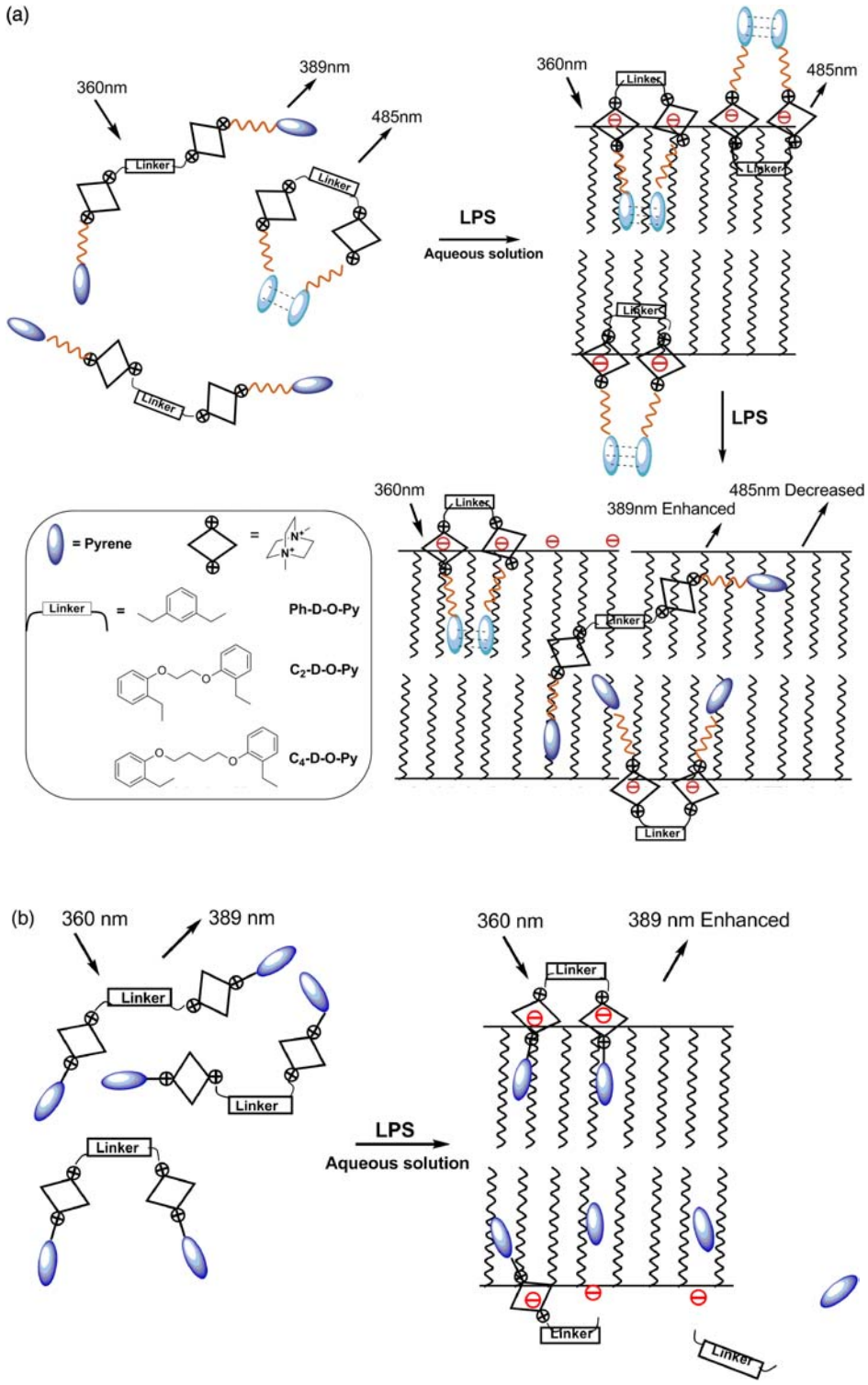

Scheme 3. The proposed schematic illustration of LPS sensing. (a) **Ph-D-O-Py**, **C_2-D-O-Py** and **C_4-D-O-Py**; (b) **C_2-D-Py**.

I_{485}/I_{389} ratio. In contrast, negligible variations of the I_{485}/I_{389} ratio were observed in the presence of Pi, pyrophosphate, sodium citrate, adenosine triphosphate (ATP), adenosine diphosphate (ADP) or adenosine monophosphate (AMP). This finding indicates that **C_4-D-O-Py** shows a sound selectivity for LPS over other simple anionic phosphates. Molecules with two carboxyl groups, including malic acid, aspartic acid and glutamic acid, cannot induce

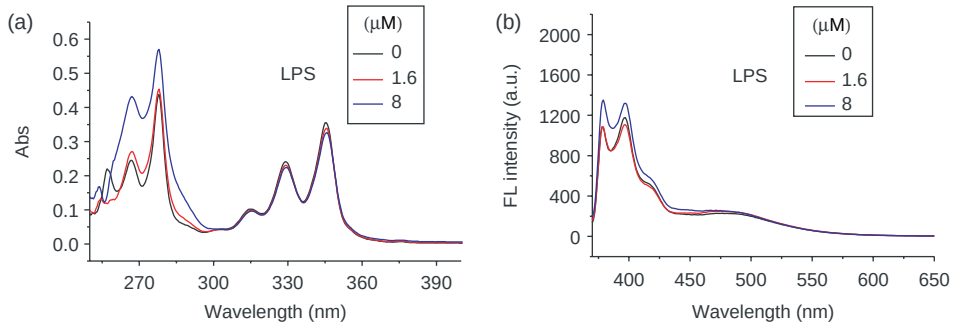

Figure 5. Spectral responses of **C_4-D-O-Py** (5.0 μM) to LPS in absolute DMSO.

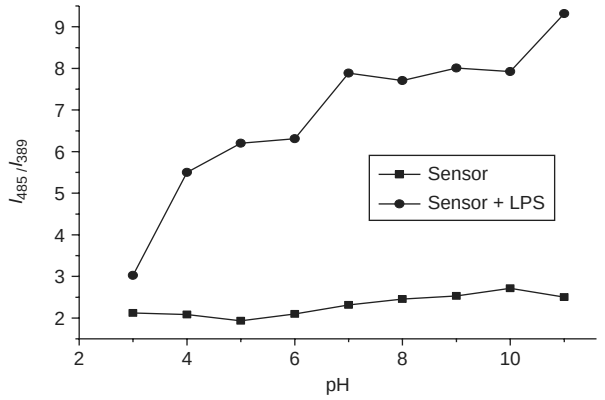

Figure 6. Effect of pH on the fluorescence intensity ratio (I_{485}/I_{389}) of free **C_4-D-O-Py** (5 μM) in the absence and presence of LPS (2.5 μM) at room temperature.

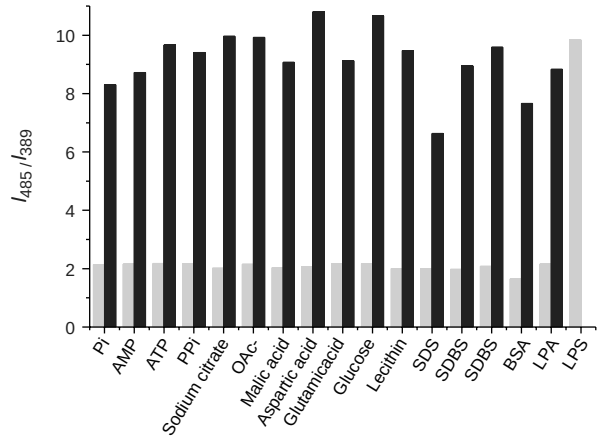

Figure 7. The selectivity of **C_4-D-O-Py** (5 μM) to LPS over competing anions or biological molecules. Grey bar: Profiles of the I_{485}/I_{389} ratio changes in a single analyte at 2.5 μM (BSA was 50 mg l^{-1}). Black bar: Profiles of normal fluorescence intensity of a mixture of competing species (2.5 μM) and LPS (2.5 μM). $\lambda_{ex} = 360$ nm.

any significant fluorescence changes in the I_{485}/I_{389} ratio. For some ordinary fatty acid salts such as sodium dodecyl sulphate and lysophosphatidic acid (LPA), although they have long alkyl chain and negatively charged end groups, they cannot induce enhancements in the I_{485}/I_{389} ratio. Moreover, **C_4-D-O-Py** shows no responses to some coexisting biomolecules in practical samples, such as glucose, albumin from bovine serum (BSA) and lecithin. In addition, **C_4-D-O-Py** exhibits an obvious enhancements of the I_{485}/I_{389} ratio to LPS even in the presence of other coexisting species, indicating that **C_4-D-O-Py** as a LPS-selective sensor is not affected by common competing species. These above results suggest evidently that **C_4-D-O-Py** shows highly selective fluorescence response for LPS in aqueous solution. As we know, LPS is highly negatively charged and more hydrophobic than other biomolecules, such as ATP, ADP, AMP, BSA and LPA. The good selectivity could be attributed to the stronger electrostatic, hydrophobic and π−π stacking interactions between the sensor and LPS, enabling them to form the supramolecular self-assembly. This selectivity results are well consistent with the sensing mechanism proposed above.

Conclusions

In summary, we have successfully developed a series of bis-pyrene derivatives bearing multi-ammonium DABCO groups as ratiometric fluorescent sensors for quantitative detection of LPS. These sensors show excellent selectivity towards LPS with tens of nanomolar sensitivity, which is the lowest value of the reported small molecule-based probes for LPS. The sensing mechanism could be suggested that the strong electrostatic and hydrophobic interactions, as well as π−π stacking of pyrene moiety induce the supramolecular self-assembly between the sensor and LPS in aqueous solution, then, if the alkyl chain between DABCO and pyrene is flexible enough to overcome the rigid conformation of DABCO groups, the overlap between the pyrene could be regulated effectively, showing a good fluorescence ratio of pyrene excimer over monomer in emission.

Experimental section

General procedures

All commercial chemicals were used without further purification. Carbon tetrachloride (CCl_4) and toluene were dried over P_2O_5 and Na, respectively. And other reagents were used as reagent grade without further purification. ^1H and ^{13}C NMR spectra were obtained on a Bruker Avance 400 NMR spectrometer using tetramethylsilane as an internal reference. EI-MS spectra were recorded on a Waters GCT Premier mass spectrometer, whereas ESI-MS on a Shimadzu LC-MS 2010 instrument. UV–vis and fluorescence spectra were measured with a Hitachi U-3010 and FL-4600 spectrometer, respectively. Fluorescence lifetime was conducted on an Edinburgh Instruments Xe-920 spectrometer. The pH measurements were carried out on a Mettler-Toledo Delta 320 pH meter.

For the spectral measurements, a stock solution (1×10^{-3} M) of sensors was prepared by dissolving 10 mmol sensors into 10 ml of DMSO. The spectrophotometic determinations of the probes, including the UV–vis spectra, fluorescence titration and selectivity, were conducted in a 10 mM HEPES buffer solution (pH 7.4; water:DMSO = 8:2, v/v).

Synthesis of 1,2-bis(o-tolyloxy)ethane (1)

Compound **1** was synthesised according to the literature with a minor modification (*18*). Sodium hydroxide (1.6 g, 40 mmol) was added into a solution of *o*-methyl phenol (2.16 g, 20 mmol) in THF (20 ml). After the mixture was refluxed for 0.5 h, 1,2-dibromoethane (1.3 g, 7 mmol) was added. The mixture was refluxed for another 48 h and concentrated by evaporation. The residue was poured into 40 ml of distilled water under stirring and then extracted with 3×15 ml of CH_2Cl_2. The combined organic layer was washed with saturated brine and dried over $MgSO_4$. The crude product was further purified by column chromatography on silica gel (ethyl acetate:petroleum ether = 5:100, v/v) to give **1** (338 mg, 20% yield) as white powder. m.p. ~87°C. ^1H NMR ($CDCl_3$, 400 MHz, δ): 7.17–7.15 (m, 4H), 6.90–6.97 (m, 4H), 4.35 (s, 4H), 2.23 (s, 6H). ^{13}C NMR ($CDCl_3$, 100 MHz, δ): 157.0, 130.9, 127.3, 126.8, 120.9, 111.5, 67.0, 16.3. HR-MS (EI) calcd for $C_{16}H_{18}O_2$ [M] 242.1307; found: 242.1302.

Synthesis of 1,4-bis(o-tolyloxy)butane (2)

The procedure for synthesis of compound **3** was similar to the process of compound **1**. Sodium hydroxide (1.6 g, 40 mmol) was added into a solution of *o*-methyl phenol (2.16 g, 20 mmol) in acetonitrile (20 ml). After the mixture was refluxed for 0.5 h, 1,4-dibromobutane (1.49 g, 7 mmol) was added. The mixture was refluxed for another 10 h. After cooling to the room temperature, the formed precipitate was filtered out and dissolved in water (40 ml). The solution was extracted with CH_2Cl_2 (3×25 ml). The combined organic layer was dried over $MgSO_4$ and concentrated to produce the crude product, which was further purified by recrystallisation from acetonitrile to yield 1.72 g (80%) of **2** as white powder. m.p. ~77°C. ^1H NMR ($CDCl_3$, 400 MHz, δ): 7.16–7.12 (m, 4H), 6.87–6.81 (m, 4H), 4.05 (t, 4H), 2.23 (s, 6H), 2.03 (m, 4H). ^{13}C NMR ($CDCl_3$, 100 MHz, δ): 157.2, 130.7, 126.9, 126.8, 120.3, 111.0, 67.5, 26.4, 16.3. MS (EI) calcd for $C_{18}H_{22}O_2$ [M] 270.1; found: 270.1.

Synthesis of compounds 3 and 4

Compounds **3** and **4** were synthesised according to reported procedures (*19*). Under a nitrogen atmosphere, a mixture of compounds **1** or **2** (1.24 mmol), *N*-bromosuccinimide (482 mg, 2.72 mmol) and azobisisobutyronitrile (60 mg) in CCl_4 (20 ml) was heated under refluxing for 1 h. After cooling to the room temperature, the reaction mixture was filtered and concentrated by evaporation. The residue was dissolved in 40 ml of CH_2Cl_2 and washed with aqueous saturated $Na_2S_2O_3$ (30 ml). The combined organic layer was dried over $MgSO_4$. The resulting crude product was further purified by column chromatography on silica gel (CH_2Cl_2:petroleum ether = 1:3, v/v) to give the dibromide derivatives as white powder.

*1,2-Bis(2,bromomethylphenoxy)ethane (**3**)*

Yield 24%, 120 mg, m.p. 122–125°C. ^1H NMR ($CDCl_3$, 400 MHz, δ): 7.35–7.29 (m, 4H), 6.99–6.94 (m, 4H), 4.56 (s, 4H), 4.47 (s, 4H). MS (EI) calcd for $C_{16}H_{16}Br_2O_2$ [M^+] 397.9; found: 397.9.

*1,4-Bis(2-(bromomethyl)phenoxy)butane (**4**)*

Yield 24%, 197 mg, m.p. ~144°C. ^1H NMR ($CDCl_3$, 400 MHz, δ): 7.34–7.26 (m, 4H), 6.93–6.88 (q, 4H), 4.58 (s, 4H), 4.15 (t, 4H), 2.13 (m, 4H). ^{13}C NMR ($CDCl_3$, 100 MHz, δ): 157.0, 130.9, 130.3, 126.3, 1207, 111.8, 67.6, 29.3, 26.2. HR-MS (EI) calcd for $C_{18}H_{20}Br_2O_2$ [M] 425.9830; found: 425.9824.

Synthesis of compounds 5 and 7

Compounds **5** and **7** were synthesised according to the previously reported procedures (*20*, *21*).

*1-(Bromomethyl)pyrene (**5**)*

Yield 24%. m.p. ~138°C. ^1H NMR ($CDCl_3$, 400 MHz, δ): 8.38(d, 1H), 8.25–8.21 (m, 3H), 8.12–8.01 (m, 5H), 5.26 (s, 2H).

*1-((4-Bromobutoxy)methyl)pyrene (**7**)*

m.p. ~215°C. ^{1}H NMR ($CDCl_3$, 400 MHz, δ): 8.36 (d, 1H), 8.14–8.22 (m, 4H), 8.00–8.07 (m, 4H), 5.22 (s, 2H), 3.64 (t, 2H), 3.41 (t, 2H), 1.98 (m, 2H), 1.82 (m, 2H).

Synthesis of compounds 6 and 8

Compounds **6** and **8** were synthesised using the same procedure. In the typical process, compound **5** (400 mg, 1.36 mmol) or **7** (497 mg, 1.36 mmol) and DABCO (182 mg, 1.50 mmol) were dissolved into 30 ml of ethyl acetate. The mixture was stirred at room temperature for 12 h and then the products were obtained by filtration.

*1-(Pyren-1-ylmethyl)-4-aza-1-azonia-bicyclo [2.2.2]octane (**6**)*

White solid (276 mg, 50%). ^{1}H NMR (CH_3OD, 400 MHz, δ): 8.55 (d, 2H), 8.36–8.33 (m, 4H), 8.26–8.11 (m, 4H), 5.30 (s, 2H), 3.56 (t, 6H), 3.14 (t, 6H). ^{13}C NMR (CH_3OD, 100 MHz, δ): 134.5, 133.2, 133.0, 132.4, 131.5, 130.6, 130.2, 128.1, 127.7, 127.5, 127.2, 126.0, 125.8, 125.2, 123.7, 120.5, 66.0, 53.6, 46.2. MS (ESI) calcd for $C_{23}H_{23}N_2^+$ [M^+] 327.1; found: 327.3.

*1-(4-(Pyren-1-ylmethoxy)butyl)-4-aza-1-azonia-bicyclo[2.2.2]octane (**8**)*

White solid (325 mg, 50%). m.p. ~120°C. ^{1}H NMR (CH_3OD, 400 MHz, δ): 8.44 (d, 2H), 8.27–8.19 (m, 4H), 8.11–8.04 (m, 4H), 5.22 (s, 2H), 3.67 (t, 2H), 2.97–2.83 (m, 14H), 1.63 (t, 2H). ^{13}C NMR (CH_3OD, 100 MHz, δ): 133.0, 132.8, 132.6, 132.0, 130.7, 128.9, 128.8, 128.6, 128.5, 127.4, 126.5, 126.4, 126.0, 125.7, 125.6, 124.9, 72.3, 69.8, 65.2, 65.1, 65.1, 53.1, 53.1, 53.1, 45.7, 27.4, 19.9. MS (MALDI) calcd for $C_{27}H_{31}N_2O^+$ [M^+] 399.2; found: 399.5.

General procedure for synthesis of the sensors

A mixture of dibromide derivatives (**3**, **4** or *m*-xylylene dibromide, 0.15 mmol) and the intermediates **6** or **8** (0.34 mmol) in appropriate amount of acetonitrile was stirred at room temperature for 12 h. The formed precipitate was filtered, washed with acetonitrile and dried under vacuum to give the desired products as pale yellow solid with moderate yield (50–70%).

*4,4′-(1,3-Phenylenebis(methylene))bis(1-(4-(pyren-1-ylmethoxy)butyl)-1,4-diazonia-bicyclo[2.2.2]octane) (**Ph-D-O-Py**)*

Yield 70%, 131 mg. m.p. ~194°C. ^{1}H NMR (DMSO, 400 MHz, δ): 8.34 (d, 2H), 8.31–8.25 (m, 8H), 8.16 (s, 4H), 8.08 (t, 4H), 7.77–7.70 (m, 4H), 5.15 (s, 4H), 4.95 (s, 4H), 4.01 (br, 12H), 3.92 (br, 12H), 3.60–3.54 (m, 8H), 1.77 (br, 4H), 1.60 (t, 4H). ^{13}C NMR (DMSO, 100 MHz, δ): 136.7, 135.6, 131.8, 130.7, 130.5, 130.2, 130.1, 128.5, 127.6, 127.3, 127.2, 126.9, 126.2, 125.3, 125.2, 124.5, 123.9, 123.8, 123.4, 70.2, 68.8, 65.6, 63.5, 50.5, 50.1, 25.9, 18.7. Element analysis: calcd for $C_{62}H_{70}Br_4N_4O_2{\cdot}2H_2O$: C, 57.51; H, 6.07; N, 4.33; found: C, 57.01; H, 5.88; N, 4.24%.

*4,4′-(2,2′-(Ethane-1,2-diylbis(oxy))bis(2,1-phenylene)) bis(methylene)bis(1-(4-(pyren-1-ylmethoxy)butyl)-1,4-diazonia-bicyclo[2.2.2]octane) (**C_2-D-O-Py**)*

Yield 60%, 125 mg. m.p. ~220°C. ^{1}H NMR (DMSO, 400 MHz, δ): 8.37 (d, 2H), 8.33–8.27 (m, 8H), 8.18–8.07 (m, 8H), 7.60–7.52 (q, 4H), 7.29 (d, 2H), 7.12 (t, 2H), 5.20 (s, 4H), 4.76 (s, 4H), 4.52 (s, 4H), 3.94 (br, 12H), 3.83 (br, 12H), 3.65 (t, 4H),3.56 (m, 4H), 1.76 (br, 4H), 1.63 (t, 4H). ^{13}C NMR (DMSO, 100 MHz, δ): 157.7, 134.9, 132.9, 131.9, 130.7, 130.5, 130.2, 128.6, 127.6, 127.3, 127.2, 126.9, 126.2, 125.3, 125.2, 124.6, 123.9, 123.8, 123.5, 121.1, 114.7, 113.2, 70.3, 68.8, 66.8, 63.1, 61.3, 50.5, 50.4, 25.9, 18.6. Element analysis: calcd for $C_{70}H_{78}Br_4N_4O_4{\cdot}2H_2O$: C, 60.27; H, 5.92; N, 4.02; found: C, 59.17; H, 5.80; N, 4.01%.

*4,4′-(2,2′-(Butane-1,4-diylbis(oxy))bis(2,1-phenylene)) bis(methylene)bis(1-(4-(pyren-1-ylmethoxy)butyl)-1,4-diazonia-bicyclo[2.2.2]octane) (**C_4-D-O-Py**)*

Yield 60%, 127 mg. m.p. ~188°C. ^{1}H NMR (DMSO, 400 MHz, δ): 8.37 (d, 2H), 8.33–8.26 (m, 8H), 8.16–8.06 (m, 8H), 7.57–7.52 (m, 4H), 7.21 (d, 2H), 7.09 (t, 2H), 5.18 (s, 4H), 4.85 (s, 4H), 4.14 (s, 4H), 3.92-3.82 (m, 24H), 3.63 (t, 4H), 3.35 (t, 4H), 2.01 (s, 4H), 1.78 (br, 4H), 1.62 (t, 4H). ^{13}C NMR (DMSO, 100 MHz, δ): 158.1, 134.8, 132.9, 131.8, 130.6, 130.5, 130.2, 128.5, 127.5, 127.3, 127.2, 126.9, 126.2, 125.3, 125.2, 124.5, 123.9, 123.8, 123.4, 120.6, 114.5, 112.9, 70.3, 68.8, 68.1, 63.1, 61.5, 50.5, 25.9, 25.3, 18.6. Element analysis: calcd for $C_{72}H_{82}Br_4N_4O_4{\cdot}2H_2O$: C, 60.77; H, 6.09; N, 3.94; found: C, 60.04; H, 6.06; N, 3.90%.

*4,4′-(2,2′-(Ethane-1,2-diylbis(oxy))bis(2,1-phenylene)) bis(methylene)bis(1-(pyren-1-ylmethyl)-1,4-diazonia-bicyclo[2.2.2]octane) (**C_2-D-Py**)*

Yield 50%, 94 mg. ^{1}H NMR (DMSO, 400 MHz, δ): 8.73 (d, 2H), 8.47–8.43 (m, 8H), 8.36 (d, 2H), 8.30–8.17 (m, 6H), 7.45 (q, 4H), 7.13 (d, 2H), 7.01 (t, 2H), 5.65 (s, 4H), 4.69 (s, 4H), 4.37 (s, 4H), 3.98 (br, 12H), 3.86 (br, 12H). ^{13}C NMR (DMSO, 100 MHz, δ): 158.2, 135.6, 134.2, 133.8, 132.9, 132.3, 131.4 130.6, 130.3, 128.0, 128.0,

127.6, 127.2, 125.9, 125.0, 124.1, 123.2, 122.1, 119.4, 114.4, 113.8, 67.3, 65.2, 63.2, 51.4. Element analysis: calcd for $C_{62}H_{62}Br_4N_4O_2{\cdot}3H_2O$: C, 58.69; H, 5.40; N, 4.42; found: C, 58.40; H, 5.57; N, 4.49%.

Supporting information

Changes of absorption and fluorescence spectra of **Ph-D-O-Py** (Figure S1) and **C_2-D-O-Py** (Figure S2) towards LPS.

Acknowledgements

This work was financially supported by the National Natural Science Foundation of China (Grant Nos 21173244 and 21073213) and the Main Direction Program of Knowledge Innovation of Chinese Academy of Sciences.

References

(1) Seltmann, G.; Holst, O. *The Bacterial Cell Wall*. Springer-Verlag, Berlin-Heidelberg.
(2) Ulevitch, R.J.; Tobias, P.S. *Curr. Opin. Immunol.* **1994**, *6*, 125–130.
(3) Raetz, C.R.H.; Whitfield, C. *Annu. Rev. Biochem.* **2002**, *71*, 635–700.
(4) Beutler, B.; Rietschel, E.T. *Nat. Rev. Immunol.* **2003**, *3*, 169–176.
(5) Raetz, C.R.H. *Annu. Rev. Biochem.* **1990**, *59*, 129–170.
(6) Van Amersfoort, E.S.; Van Berkel, T.J.C.; Kuiper, J. *Clin. Microbiol. Rev.* **2003**, *16*, 379–414.
(7) Roslansky, P.F.; Novitsky, T.J. *J. Clin. Microbiol.* **1991**, *29*, 2477–2483.
(8) Zhang, G.H.; Baek, L.; Nielsen, P.E.; Buchardt, O.; Koch, C. *J. Clin. Microbiol.* **1994**, *32*, 416–422.
(9) Kim, S.K.; Lee, D.H.; Hong, J.I.; Yoon, J. *Accounts Chem. Res.* **2009**, *42*, 23–31.
(10) Wu, J.; Liu, W.; Ge, J.; Zhang, H.; Wang, P. *Chem. Soc. Rev.* **2011**, *40*, 3483–3495.
(11) Rangin, M.; Basu, A. *J. Am. Chem. Soc.* **2004**, *126*, 5038–5039.
(12) Voss, S.; Fischer, R.; Jung, G.; Wiesmuller, K.H.; Brock, R. *J. Am. Chem. Soc.* **2007**, *129*, 554–561.
(13) Ganesh, V.; Bodewits, K.; Bartholdson, S.J.; Natale, D.; Campopiano, D.J.; Mareque-Rivas, J.C. *Angew. Chem. Int. Edit.* **2009**, *48*, 356–360.
(14) Wu, J.; Zawistowski, A.; Ehrmann, M.; Yi, T.; Schmuck, C. *J. Am. Chem. Soc.* **2011**, *133*, 9720–9723.
(15) Lan, M.; Wu, J.; Liu, W.; Zhang, W.; Ge, J.; Zhang, H.; Sun, J.; Zhao, W.; Wang, P. *J. Am. Chem. Soc.* **2012**, *134*, 6685–6694.
(16) Zeng, L.T.; Wang, P.F.; Zhang, H.Y.; Zhuang, X.Q.; Dai, Q.; Liu, W.M. *Org. Lett.* **2009**, *11*, 4294–4297.
(17) Sun, J.Y.; Ge, J.C.; Liu, W.M.; Wang, X.L.; Fan, Z.Y.; Zhao, W.W.; Zhang, H.Y.; Wang, P.F.; Lee, S.T. *Nano Res.* **2012**, *5*, 486–493.
(18) Cope, A.C. *J. Am. Chem. Soc.* **1935**, *57*, 572–574.
(19) Black, D.S.C.; Horsham, M.A.; Rose, M. *Tetrahedron* **1995**, *51*, 4819–4828.
(20) Xu, Z.; Singh, N.J.; Lim, J.; Pan, J.; Kim, H.N.; Park, S.; Kim, K.S.; Yoon, J. *J. Am. Chem. Soc.* **2009**, *131*, 15528–15533.
(21) Dai, Q.; Liu, W.; Zhuang, X.; Wu, J.; Zhang, H.; Wang, P. *Anal. Chem.* **2011**, *83*, 6559–6564.